

---

---

# Interior Insulation Retrofit of a Brick Wall Using Vacuum Insulation Panels: Design of a Laboratory Study to Determine the Hygrothermal Effect on Existing Structure and Wooden Beam Ends

Pär Johansson

Berit Time, PhD

Stig Geving, PhD

Bjørn Petter Jelle, PhD

Angela Sasic Kalagasidis, PhD

Carl-Eric Hagentoft, PhD

Egil Rognvik

## ABSTRACT

*The increasing demand on energy-efficient buildings requires energy retrofitting measures in the existing building stock. Conventional thermal insulation materials, such as mineral wool and expanded polystyrene (EPS), demand a thick layer of insulation to reach the energy targets. Vacuum insulation panels (VIPs) are a novel thermal insulation component with 5–10 times lower thermal conductivity than the conventional insulation materials, depending on the VIP ageing state. The thermal transmittance of the building envelope can thereby be substantially reduced using a limited additional insulation thickness. Previous research has shown that interior energy retrofitting of exterior walls may increase the moisture content of the walls and increases the risk of freeze-thaw damages at the surface. This study analyzes the hygrothermal consequences on a 250 mm (9.8 in.) thick brick wall retrofitted with 20 mm (0.8 in.) interior VIP (glued directly on the plastered brick wall). Hygrothermal simulations in WUFI 2D are used to study the hygrothermal effects by different material properties and boundary conditions. Apart from the material properties, the amount of driving rain available at the surface is the most important influential parameter in the simulations. The conclusions from this study are used to plan a measurement study in a climate simulator where driving rain and solar radiation will be simulated.*

## INTRODUCTION

One of the main challenges in the building sector is to reduce the energy use in the existing building stock. In Sweden, 47% of the building stock is from before 1960. These buildings are the ones with the highest average thermal transmittance of the exterior wall,  $0.58 \text{ W}/(\text{m}^2 \cdot \text{K})$  ( $\text{R}-10 \text{ ft}^2 \cdot ^\circ\text{F} \cdot \text{h}/\text{Btu}$ ), compared to  $0.44 \text{ W}/(\text{m}^2 \cdot \text{K})$  ( $\text{R}-13 \text{ ft}^2 \cdot ^\circ\text{F} \cdot \text{h}/\text{Btu}$ ) for all the existing buildings in Sweden (Boverket 2009). In Oslo, the capital of Norway, there are 3000 brick buildings built between 1800 and 1900. Their technical characteristics and guidelines to how they should be maintained are described by Bjørberg et al. (2011). Many of these buildings are protected for their architectural qualities. The Swedish board of housing and planning, Boverket, estimates that 41% of the buildings in the Swedish building stock are not suitable for exterior retrofitting of the façade and 28% are considered dubious (Boverket 2010). The situation in Norway is somewhat similar,

though there are no reports available analyzing the building stock with regard to suitability for interior or exterior insulation. However, it is known that about 100 000 multifamily buildings were built before 1945, with an average thermal transmittance of the exterior wall of  $0.9 \text{ W}/\text{m}^2 \cdot \text{K}$  ( $\text{R}-6.3 \text{ ft}^2 \cdot ^\circ\text{F} \cdot \text{h}/\text{Btu}$ ) (Thyholt et al. 2009). The façades of many of these buildings are likely protected for their architectural qualities. Hence, a majority of the buildings will not be possible to retrofit on the exterior and other energy efficiency measures have to be used instead.

Retrofitting of an exterior wall changes the hygrothermal performance of the wall, which could lead to damages and, in the worst case, building failure. When adding insulation to the exterior of the wall, the existing structure is kept in a warm and dry condition, which is beneficial from a building physics point of view. Listed buildings whose features and aesthetics are to be preserved (see Figure 1a for an example of

---

*Pär Johansson is a doctoral student, Angela Sasic Kalagasidis is an assistant professor, and Carl-Eric Hagentoft is a professor at Chalmers University of Technology, Sweden. Berit Time is a senior scientist at SINTEF Building and Infrastructure, Norway. Stig Geving is a professor at Norwegian University of Science and Technology, Norway. Bjørn Petter Jelle is a professor at Norwegian University of Science and Technology and a senior scientist at SINTEF Building and Infrastructure. Egil Rognvik is an engineer at SINTEF Building and Infrastructure.*



**Figure 1** (a) An old industrial building considered to have a façade with special aesthetic values that should be preserved and (b) a connection between a wooden beam and brick wall.

such a building) cannot be insulated on the exterior. In these cases interior insulation is the only option to reduce the heat losses through the exterior walls. Interior insulation of walls is a topic that has been investigated continuously during the years. Straube et al. (2011) studied a number of brick buildings in the U.S. to which interior insulation had been added and concluded that rainwater has to be treated properly and that there is a risk that wooden beam ends in the walls (see Figure 1b) may be damaged. Künzle (1998) showed that exterior walls insulated on the interior need to be combined with rain protection measures to avoid moisture-induced damages.

The thickness of the additional interior insulation layer is an important limitation because the rentable floor area will be reduced after the retrofit. Materials with a lower thermal conductivity make it possible to reduce the thermal transmittance while minimizing the rentable floor area reduction. Vacuum insulation panels (VIPs) are a novel thermal insulation component with 5–10 times lower thermal conductivity than the conventional insulation materials (Baetens et al. 2010) such as mineral wool and expanded polystyrene (EPS), depending on the VIP ageing state. Sveipe et al. (2011) showed that the VIP may represent a condensation risk when used on the exterior. They investigated timber frame walls with 100 mm (3.9 in.) mineral wool and 20–30 mm (0.8–1.2 in.) VIP in laboratory experiments. The walls lacked an interior vapor barrier. The exterior climate was  $-18^{\circ}\text{C}$  ( $-0.4^{\circ}\text{F}$ ) with 60% relative humidity and the interior climate was  $20^{\circ}\text{C}$  ( $68^{\circ}\text{F}$ ) with 50%–60% relative humidity, i.e., there was a moisture excess of  $8\text{--}10\text{ g/m}^3$  ( $100\text{--}130\text{ lb/ft}^3$ ). With these boundary conditions, the vapor in the air could reach the saturation vapor content and condense on the cold surfaces. However, with a vapor barrier on the interior this problem could have been

avoided but a new moisture problem could arise where moisture is trapped between the interior vapor barrier and the exterior VIP.

The decreasing heat resistance of the VIP during many years of use, due to diffusion of water vapor and air through the enclosing VIP laminate (Baetens et al. 2010; Wegger et al. 2011), also represents a calculation challenge when studying VIPs. Pfluger et al. (2008) used hygrothermal simulations, laboratory investigations, and field tests to investigate interior insulation retrofit of walls using VIPs. The results showed that interior insulation with VIPs is possible without causing moisture-induced damages as long as the attachment details are designed to minimize air leakage from the interior and the façade is protected from driving rain.

This paper presents one- and two-dimensional simulations performed in WUFI 2D (Fraunhofer IBP 2010) with the purpose of preparing an experimental benchmark in a laboratory environment where a brick wall with wooden beam ends is insulated with VIPs on the interior. The goal is to propose design conditions for a measurement procedure and for the design of retrofit solutions to minimize the risk of damages to the existing structure. Special focus is pointed at investigating the influence of the retrofitting on the wooden beam ends and practical limitations when using VIPs. Wooden beam ends are studied because this is a known risk area when insulating brick buildings on the interior. The study is part of a research project run in cooperation with Chalmers University of Technology in Gothenburg, Sweden, and the Norwegian University of Science and Technology and SINTEF Building and Infrastructure in Trondheim, Norway. A laboratory investigation where a brick wall was exposed to varying conditions in a climate simulator following the results of the simulations presented in this paper was performed in January to June 2013.

## INTERIOR RETROFIT RISKS

The brick walls that are targeted for this study are normally 1.5 bricks thick—380 mm (15 in.)—which is a common wall thickness in buildings from the late 19th century (Kvande and Edvardsen 2007). The walls often have a wooden beam inserted around 200 mm (8 in.) into the brick (see Figure 2). When the wall is insulated on the interior, the beam end will be in a colder environment. Rasmussen (2010) used numerical simulations to find the change in temperature of the wooden beams when retrofitted on the interior and concluded that the temperature was substantially reduced. With 95 mm (3.7 in.) mineral wool, an interior temperature of 20°C (68°F), and 0°C (32°F) at the exterior, the temperature could be reduced from 10°C to 7°C (50°F to 45°F) after the wall is insulated. If the moisture load is constant, the relative humidity at the coldest point will increase, thus increasing risk of mold growth and rot in the beam.

Brick walls are capillary active, which means they will absorb water from driving rain until the surface layer is fully covered by a water film and the water runs down along the façade. The influence of driving rain on a brick wall insulated on the interior with 200 mm (8 in.) mineral wool was investigated numerically by Morelli et al. (2010). The influence by the amount of water available for capillary absorption was studied using the coupled heat and moisture program DELPHIN (Nicolai et al. 2013). A rain shielding factor between 0.1 and 0.5 was investigated in the study. When the façade was fully protected and no capillary absorption took place the factor was 0; if all the rain was available for capillary absorption the factor was 1. The driving rain showed to have a major influence on the performance of the wall where the relative humidity at the beam end was studied in detail. The additional

thermal insulation reduced the temperature in the wall, thus elevating the relative humidity in the wooden parts, leading to risk for moisture damages. It was shown that the high moisture content in the wooden beam end could be reduced by enlarging the thermal bridge around the wooden beam by removing 300 mm (12 in.) of the insulation above and below the wooden beam, as shown by the horizontal black lines in Figure 2. Using this measure, the relative humidity of the beam end was decreasing from its starting value of 85%. However, with a rain shielding factor of 0.5 instead of 0.1, the relative humidity increased to more than 95%.

The movement of water through brick masonry has many important consequences in building construction and has therefore been studied by a number of authors, e.g., Hall (1977) and Brocken (1998). While the majority of these studies involved water suction experiments from a free water surface, large-scale experiments where water suction in brick walls is studied during a real or artificial rain load, such as presented by Abuku et al. (2009) and Piaia et al. (2013), are rare. To the knowledge of the authors, similar studies for brick masonry are not readily available.

Also, bricks that are not freeze-thaw resistant can be damaged if too-high moisture levels occur in the wall during freeze-thaw cycles. The water in the capillaries of the brick expands when it freezes, and after a number of cycles the structure starts to disintegrate. Mensinga et al. (2010) studied the risk of frost damage on bricks subjected to freeze-thaw cycles in a retrofitted wall. A risk assessment methodology based on frost dilatometry was developed where the critical level of moisture saturation for freeze-thaw damage could be found. They experienced that the critical degree of saturation (defined as the ratio of the moisture content over the moisture content when all accessible pores are filled with water) varied from 0.25 to 0.8 for two different investigated types of brick. This information is important when deciding on the retrofit design of the brick wall to ensure a safe moisture state in the brick.

When using VIPs it is essential to ensure airtight connections between the panels to avoid any convective moisture transfer into the wall from the interior of the building. Old brick walls can be damaged internally with cracks in the brickwork and mortar, which could mean the moist indoor air can be transferred into the colder parts of the construction and eventually condense. It is also important to make sure the moisture content in the wall close to the VIPs is not too high, since it has not yet been entirely evaluated how the panels can handle a longer exposure to a moist environment. Brunner et al. (2008) studied the formation of soluble aluminum oxide and transparent aluminum oxide in the enclosing VIP laminate by high heat and moisture load. In accelerated ageing experiments representative of 25 years of normal exposure, aluminum oxides did not form. If aluminum oxides formed in the VIP laminate, the diffusion of water vapor and air through the laminate would increase the thermal conductivity to

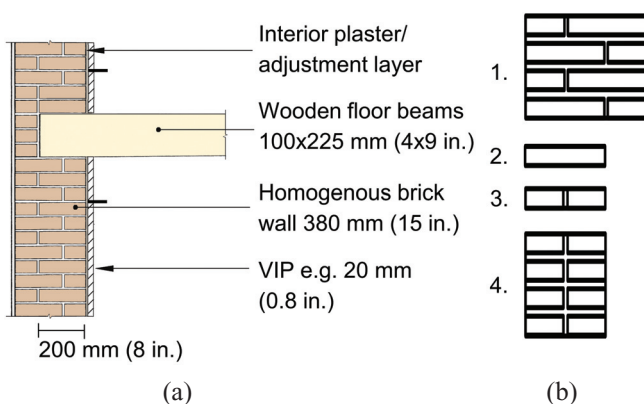


**Figure 2** (a) Schematics of a brick wall with a wooden floor beam inserted in the brick wall (© 2013 SINTEF) where the black horizontal lines through the insulation layer mark the 300 mm (12 in.) gap in the insulation described by Morelli et al. (2010) and (b) the simulated cases of brick and mortar investigated in this paper.

around half the thermal conductivity of conventional insulation materials.

### HYGROTHERMAL SIMULATIONS

In this study one- and two-dimensional hygrothermal simulations are used to investigate the hygrothermal performance of a masonry wall based on the following parameters:

- Climate: temperature, relative humidity, solar radiation, and driving rain
- Climate load at the location of the wall
- Wall thickness
- Type of brick
- Type of mortar
- Internal thermal insulation

The investigation starts with an analysis of the climate at the location of the building. The climates of Bergen (west coast of Norway) and Gothenburg (west coast of Sweden) are compared since these are the cities with the highest driving rain loads in Norway and Sweden. Figure 3 shows the temperature and relative humidity in Bergen and Gothenburg.

As can be seen, the climates in Bergen and Gothenburg are very similar, with average yearly temperatures of 8.1°C and 8.8°C (46.6°F and 47.8°F), respectively. The average relative humidity is 80.6% in Bergen and 74.5% in Gothenburg. The annual rainfall in Bergen is 2 421 mm (95.3 in.) and in Gothenburg is 1 074 mm (42.3 in.). Both cities are located close by the sea, which means a large portion of driving rain hits the façades of the buildings.

The measurement study should be based on real climate data to simulate the behavior of a future full-scale retrofitting measure. However, the climate simulator has some limitations and there is a time limitation for how long each test sequence can be run. The climate simulator generates a controlled dynamic climate condition on both sides of the

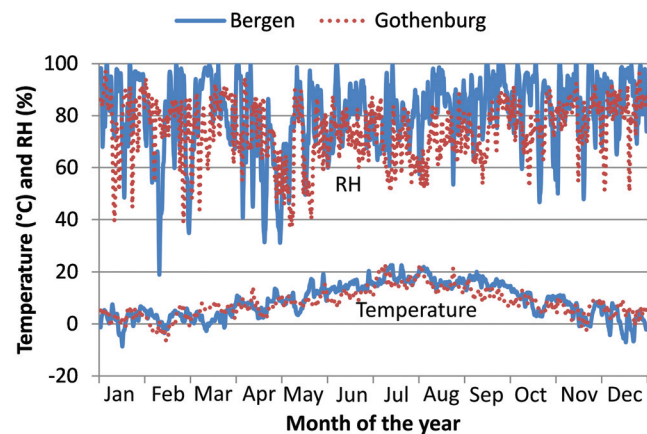


**Figure 3** Temperature and relative humidity in Bergen (solid line) compared to Gothenburg (dotted line) starting with January based on data from WUFI 2D (Fraunhofer IBP 2010).

brick wall. On the exterior side of the chamber, the climate can be set to vary between  $-20^{\circ}\text{C}$  and  $+80^{\circ}\text{C}$  ( $-4^{\circ}\text{F}$  and  $+176^{\circ}\text{F}$ ) with a relative humidity of 20%–95%. The rain hitting the test wall is produced by a set of nozzles able to produce 15–35  $\mu\text{m}$  (590–1380  $\mu\text{in.}$ ) large droplets with a rain intensity of 10–100 mm/h (0.39–3.9 in./h). Nine metal halide global lamps produce an artificial solar radiation with a wavelength distribution similar to that of natural solar radiation. The maximum solar intensity is  $1000 \text{ W/m}^2$  (3412 Btu/h), which can be controlled continuously between 50% and 100%. On the interior side of the wall the temperature can be varied between  $+5^{\circ}\text{C}$  and  $+50^{\circ}\text{C}$  ( $41^{\circ}\text{F}$  and  $122^{\circ}\text{F}$ ) with a relative humidity of 20%–95% (Angelantoni Industries S.p.A., n.d.).

### Climate Load on the Location of the Wall

The moisture conditions in 380 mm (15 in.) brick walls in Bergen and Gothenburg with the material data of extruded brick and coarse lime cement mortar defined in Table 1 were simulated with two-dimensional heat and moisture transfer. The sorption isotherms of the bricks included in this study are presented in Figure 4. The thermal conductivity and specific heat capacity of the brick and mortar are  $0.6 \text{ W/(m}\cdot\text{K)}$

**Table 1. Material Data for the Hygrothermal Simulations of Four Brick Types and Six Mortar Types based on Data from WUFI 2D (Fraunhofer IBP 2010)\***

Material	Density, $\text{kg/m}^3$	Porosity	Water Vapor Diffusion Resistance Factor	Liquid Water Transfer Coefficient, $\text{m}^2/\text{s}$
Masonry brick	1900	0.24	10	1.7
Extruded brick	1650	0.41	9.5	70
Hand-formed brick	1725	0.38	17	200
Historical brick	1800	0.31	15	300
Cement (C) type S mortar	1885	0.50	15.5	0.00075
Cement (C) type N mortar	1885	0.50	14.8	0.0015
Coarse lime cement (LC) mortar	1910	0.25	46	0.87
Fine lime cement (LC) mortar	1880	0.28	50	0.31
Coarse hydraulic lime (L) mortar	1830	0.27	20	0.9
Fine hydraulic lime (L) mortar	1700	0.35	14.8	0.33

\* The sorption isotherms of the bricks included in this study are presented in Figure 4.

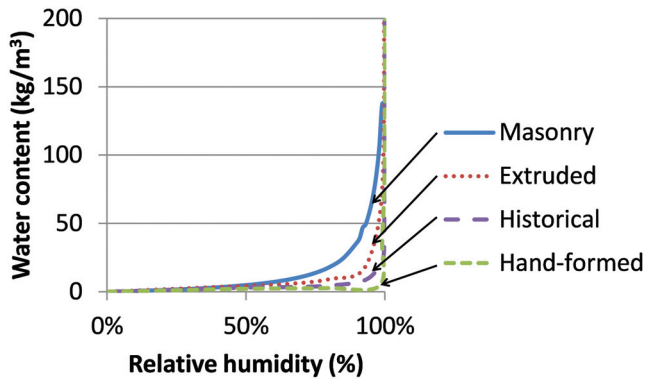


**Figure 4** Sorption isotherms at 23°C of the four types of brick included in the study based on data from WUFI 2D (Fraunhofer IBP 2010).

(0.35 Btu/[h·ft·°F]) and 850 J/(kg·K) (0.2 Btu/[lb·°F]), respectively. The initial conditions of the materials were 15°C (59°F) and 70% relative humidity. The sizes of the bricks were 250 × 120 × 62 mm (9.8 × 4.7 × 2.4 in.) and the thicknesses of the mortar joints between the bricks were 10–12 mm (0.39–0.47 in.) (see number 1 in Figure 2). On the interior, the climate is defined by EN 15026 (CEN 2007) with a normal moisture load. The interior heat transfer coefficient,  $h$ , is 8 W/m<sup>2</sup>·K (R-0.7 ft<sup>2</sup>·°F·h/Btu), and the interior diffusion equivalent air layer thickness,  $sd$ , is 3 m (1.1 perm). The  $sd$  value describes the resistance to moisture transfer by the surface material in terms of equivalent air thickness. The rainwater hitting the façade, available for capillary absorption, is determined by the rainwater absorption factor. When the façade is fully protected and no capillary absorption takes place the factor is 0, and if all the rain is available for capillary absorption the factor is 1. In WUFI 2D, a rainwater absorption factor of 0.7 is considered to be adequate for normal walls (Fraunhofer IBP 2010). The dominant wind direction for both Bergen and Gothenburg is south, which therefore was chosen as the direction the wall is facing. The wall is considered to be protected from most of the rain with a rain water absorption factor of 0.3. The exterior heat transfer coefficient is 25 W/m<sup>2</sup>·K (R-0.2 ft<sup>2</sup>·°F·h/Btu). The results are shown in Figure 5.

In Bergen, the resulting relative humidity in the middle of the wall is close to 100% after only 1 year of simulation. Also, the water content in the middle of the wall increases rapidly during the first years of the simulation, stabilizing during years 4 and 5. The moisture is evenly distributed in the wall. The maximum water content is 147 kg/m<sup>3</sup> (9 lb/ft<sup>3</sup>) in December of year 4, while the saturation moisture content is 370 kg/m<sup>3</sup> (23 lb/ft<sup>3</sup>). At the surface of the brick, where there could be risk of freeze-thaw damages, the moisture content is significantly higher, peaking at 298 kg/m<sup>3</sup> (19 lb/ft<sup>3</sup>). The degree of saturation becomes 0.4 at maximum, and the number of freeze-thaw cycles during the simulated year is 16. However, the critical degree of saturation is not known for the brick used in the simulations. As mentioned previously, measurements have shown that the critical degree of saturation can be in the

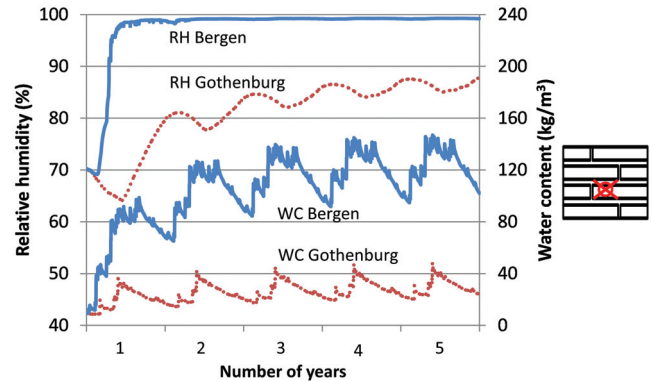


**Figure 5** Relative humidity in the middle of a 380 mm (15 in.) thick homogenous brick wall (marked by a cross with circle in the right figure) and total water content in the wall, which is made of extruded brick and coarse lime cement mortar. The wall is facing south in both Bergen and Gothenburg with a 0.3 rainwater absorption factor.

range of 0.25–0.8 (Mensinga et al. 2010). Investigation of the critical degree of saturation for the specific brick used in the wall to be retrofitted has to be determined to conclude the risk for freeze-thaw damages.

In Gothenburg the brick wall is also be exposed to driving rain; however, the rain load is not as high as it is in Bergen. The relative humidity peaks at 88% in the middle of the wall in August of year 5. The water content in the middle of the wall is only 48 kg/m<sup>3</sup> (3 lb/ft<sup>3</sup>) at maximum while it is 211 kg/m<sup>3</sup> (13 lb/ft<sup>3</sup>) at the exterior surface of the brick wall. The moisture content is highest in the exterior part of the wall. The degree of saturation becomes 0.13, which should be below the critical degree of saturation for most brick types. Although, the number of freeze-thaw cycles in a year in Gothenburg is 35, which is much higher than that in Bergen. The combination of many freeze-thaw cycles and unprotected brick façades could explain why many brick buildings in Gothenburg have freeze-thaw damage. If the wall is not protected from driving rain, the moisture content in the middle of the wall will be very high, even in its original state.

### Wall Thickness

One-dimensional hygrothermal simulations are used to estimate how long of a testing period the full wall thickness would require to notice the moisture accumulation in the wall. The hypothesis is that the same hygrothermal mechanisms will take place in the wall independent of the thickness. Only the time scale will be influenced by a reduced thickness in the laboratory study. Figure 6 shows the relative humidity 60 mm (2.4 in.) from the interior of the wall in two brick walls of three different thicknesses. In this part of the study it is the influence of the bricks only that is of interest; therefore, no mortar was simulated between the bricks (see number 2 in

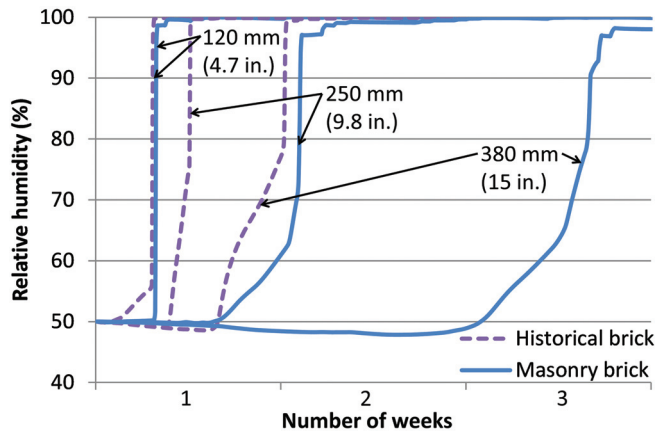


**Figure 6** Relative humidity 60 mm (2.4 in.) from the interior surface of the two brick walls with varying thicknesses composed of homogenous historical bricks and masonry bricks as defined in Table 1 and during the climate cycle defined in Table 2.

Figure 2). The walls are composed of homogenous historical bricks and masonry bricks and are defined in Table 1. The initial conditions of the materials are 20°C (68°F) and 50% relative humidity. The interior climate is 20°C (68°F) and 40% relative humidity. The interior heat transfer coefficient is 8 W/m<sup>2</sup>·K (R-0.7 ft<sup>2</sup>·°F·h/Btu) and the interior *sd* value is 0.2 m (16 perm). The exterior climate is defined in Table 2, which is based on the HAMSTAD Benchmark Project (Hagentoft et al. 2004) where the moisture accumulation in a brick wall was studied during a climate cycle of heavy rainfall with drying periods in between. Note that this is a fictitious climate where the exterior relative humidity is fixed at 90%. The hours with rainfall are limited, which means the drying during these hours is limited compared to the wetting by the rain and the drying during the hours without rain. The exterior heat transfer coefficient is 25 W/m<sup>2</sup>·K (R-0.2 ft<sup>2</sup>·°F·h/Btu) with a wind-dependent vapor resistance. The wall is facing the dominant wind direction towards the south with a rain water absorption factor of 1; i.e., all rain is available for capillary absorption.

The time before the wall reaches saturation 60 mm (2.4 in.) from the interior surface of the brick wall is different depending on the thickness of the wall and the type of bricks in the wall. For the 120 mm (4.7 in.) thick historical brick wall it takes 53 hours, for the 250 mm (9.8 in.) thick wall it takes 87 hours, and for the 380 mm (15 in.) thick wall it takes 173 hours. It takes a longer time for the masonry brick wall to reach saturation. For the 120 mm (4.7 in.) thick wall it takes 64 hours, for the 250 mm (9.8 in.) thick wall it takes 218 hours, and for the 380 mm (15 in.) thick wall it takes 578 hours. The relation is not linear between the thickness and moisture accumulation. For the thinnest historical brick wall the moisture condensates after 30% of the time for the thickest wall, while it takes 11% of the time for the masonry

**Table 2. Exterior Climate for Wetting of Brick Wall in a 120 Hour Cycle\***

Duration, h	Rain, mm	Sun, W/m <sup>2</sup>	Exterior Temperature, °C	Exterior Relative Humidity, %
6	0	0	10	90
16	0	0	-2	90
27	0	0	10	90
6	2	0	10	90
7	0	0	10	90
4	2.5	0	10	90
6	0	0	10	90
7	0	1000	10	90
5	0	0	10	90
4	2	0	10	90
7	0	1000	10	90
3	3	0	10	90
8	0	1000	10	90
4	2	0	10	90
10	0	0	10	90

\* Based on the climate used in the HAMSTAD Benchmark Project (Hagentoft et al. 2004).

brick wall; the thickness is 32% of the thickest wall. In the middle wall, 250 mm (9.8 in.), the moisture condensates after 50% of the time for the historical brick, while it takes 38% of the time for the masonry brick wall; the thickness is 66% of the thickest wall. Despite the differences in the time of wetting, the moisture levels in the walls are at the same level at the end of the simulation and thus it is concluded that a thinner wall can be used in the experiment but the time scale has to be decided based on the permeability of the bricks.

### Type of Brick

In previous research, it was found that the type of brick is very important to the test results; modern bricks are less capillary active than the hand-formed bricks manufactured many years ago (Hammett 1997). The main difference between the four bricks given in Table 1 is the liquid water transfer coefficient, which varies from 1.7 to 300 m<sup>2</sup>/s (0.2 to 27.9 ft<sup>2</sup>/s). For the masonry and extruded bricks, the liquid transfer is lower than for the hand-formed and historical bricks. The sorption isotherms of the bricks included in this study are presented in Figure 4.

Figure 7 shows the results from one-dimensional simulations of the moisture accumulation in a 250 mm (9.8 in.)

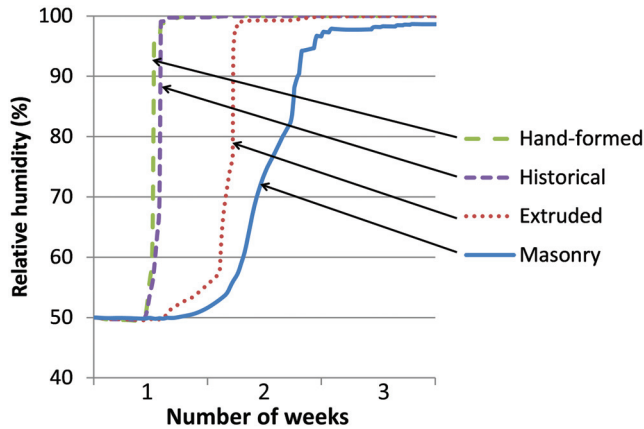


**Figure 7** Relative humidity 60 mm (2.4 in.) from the interior surface of the 250 mm (9.8 in.) brick wall with one of the brick types and fine lime cement mortar from Table 1 during the climate cycle defined in Table 2.

brick wall with one of the four different brick types in Table 1. There is a layer of fine lime cement mortar in the middle of the wall to simulate the real case of a wall with two bricks placed next to each other (see number 3 in Figure 2). The initial conditions and boundary conditions are the same as in the previous section.

The difference between the bricks is clear, and the four types of brick tested can be divided into two main groups where the historical and hand-formed bricks are similar while the extruded and masonry bricks are less similar. The time before the walls are saturated with moisture at the point 60 mm (2.4 in.) from the interior differs from 99 and 108 hours for historical and hand-formed bricks to 217 hours for extruded brick and 588 hours for masonry. These differences confirm that it is important to investigate the properties of the specific type of bricks used in the study to be able to predict the results of the laboratory study.

### Type of Mortar

The type of mortar also influences the moisture properties of the wall. To investigate the time required for drying the wall during the laboratory investigations, a wall was placed indoors in the laboratory environment and the drying period was investigated. The material data for the six different mortars are given in Table 1. The main difference between the mortars is the liquid water transfer coefficient, which is substantially larger for the lime cement mortars and hydraulic lime mortars compared to the pure cement mortar. In the early 20th century, lime mortar was used in masonry buildings. Pure lime mortar requires a longer time for curing than a mixture of lime and cement. The difference between cement types S and N is in the final strength. Type S has higher final strength than type N, which is the type normally recommended for masonry work (BIA 2006). Figure 8 shows the

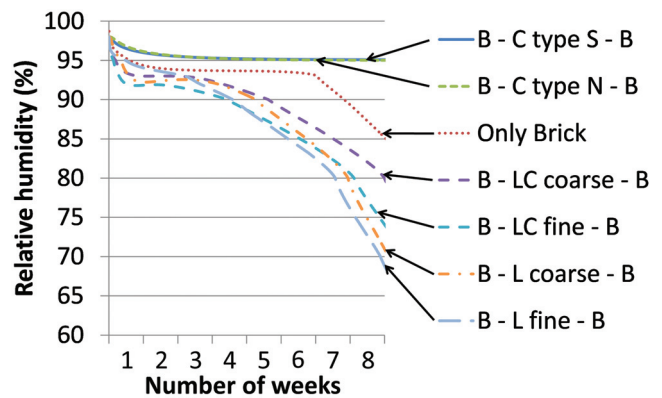


**Figure 8** Relative humidity in the middle of the mortar in a 250 mm (9.8 in.) extruded brick (B) wall with varying mortar properties placed indoors in Trondheim, Norway, starting on October 1 based on data from the WUFI database (Fraunhofer IBP 2010). For comparison, a wall with only brick is simulated under the same conditions.

drying time for a wall dependent on the type of mortar used in a 250 mm (9.8 in.) thick wall with the extruded brick from Table 1 and a 10–12 mm (0.39–0.47 in.) thick mortar layer between the bricks with two-dimensional heat and moisture transfer (see number 4 in Figure 2). The starting condition is a fully saturated mortar at 20°C (68°F) and brick with 80% relative humidity. The interior climate is 20°C (68°F) and 40% relative humidity. The interior heat transfer coefficient is 8 W/m<sup>2</sup>·K (R-0.7 ft<sup>2</sup>·°F·h/Btu) and there is no surface coating applied. The wall is fully exposed to the indoor climate of the laboratory in Trondheim, Norway, to simulate the drying during the period starting on October 1 with a normal moisture load defined by EN 15026 (CEN 2007). For comparison, a wall of only brick is simulated in the same conditions.

Pure cement mortar (C) gives a very slow drying process, and after 8 weeks the relative humidity in the wall has only been reduced by 3 percentage points, to 95%. For the other mortar types, the drying is much faster. The fastest is for the fine hydraulic lime mortar (L), where the relative humidity is reduced to 70% after 8 weeks of drying. The coarse and fine types of the mortars have different properties as well, but the difference in relative humidity is not as large after 8 weeks as when comparing the lime cement mortar (LC) and hydraulic lime mortar (L). The wall with only brick has a slow drying during the first 6 weeks, but thereafter it dries quickly, down to 83% after 8 weeks. The influence of the mortar is that it shortens the drying process of the wall, which could be explained by a higher moisture transport through the thinner capillaries of the mortar than through the coarser brick capillaries. This could also have an influence during the wetting phase of the walls with different thicknesses, described previously. However, as Figure 8 shows, the difference is limited

between the wall with only brick and the different mortars. For the forthcoming laboratory study, a mixture of lime and cement will be used as mortar.

### Internal Thermal Insulation

The thermal conductivity of pristine VIP is below  $5 \text{ mW}/(\text{m}\cdot\text{K})$  (R-29 per in.) but increases, due to diffusion of water vapor and air through the enclosing VIP laminate, to around  $7$  or  $8 \text{ mW}/(\text{m}\cdot\text{K})$  (R-18-21 per in.) in 25 years (Brunner and Simmler 2008). The VIPs investigated in this study are pristine, which is why the lower thermal conductivity of  $5 \text{ mW}/(\text{m}\cdot\text{K})$  (R-29 per in.) was chosen.

The VIPs have a very high vapor resistance compared to, for example, mineral wool insulation. On the other hand, the gaps between the panels can be around  $2$  to  $4 \text{ mm}$  ( $0.08$  to  $0.16 \text{ in.}$ ), which could allow vapor transfer. To investigate this, four cases are studied more in detail:

1. Original brick wall;  $h = 8 \text{ W}/\text{m}^2\cdot\text{K}$  (R-0.7  $\text{ft}^2\cdot\text{F}\cdot\text{h}/\text{Btu}$ ),  $sd = 0.2 \text{ m}$  (16 perm)
2. Vapor barrier on the interior;  $h = 8 \text{ W}/\text{m}^2\cdot\text{K}$  (R-0.7  $\text{ft}^2\cdot\text{F}\cdot\text{h}/\text{Btu}$ ),  $sd = 1500 \text{ m}$  (0.002 perm)
3. Vapor-open insulation with a heat resistance equivalent to  $20 \text{ mm}$  ( $0.8 \text{ in.}$ ) VIP;  $h = 0.242 \text{ W}/\text{m}^2\cdot\text{K}$  (R-235  $\text{ft}^2\cdot\text{F}\cdot\text{h}/\text{Btu}$ ),  $sd = 0.2 \text{ m}$  (16 perm)
4. Interior insulation with  $20 \text{ mm}$  ( $0.8 \text{ in.}$ ) VIP;  $h = 0.242 \text{ W}/\text{m}^2\cdot\text{K}$  (R-235  $\text{ft}^2\cdot\text{F}\cdot\text{h}/\text{Btu}$ ),  $sd = 1500 \text{ m}$  (0.002 perm)

The original wall is  $250 \text{ mm}$  ( $9.8 \text{ in.}$ ) thick with the historical brick from Table 1 and a  $10 \text{ mm}$  ( $0.39 \text{ in.}$ ) thick layer of fine lime cement mortar between the bricks as shown in number 3 in Figure 2. The initial conditions of the materials are  $20^\circ\text{C}$  ( $68^\circ\text{F}$ ) and  $50\%$  relative humidity. The interior cli-

mate is  $20^\circ\text{C}$  ( $68^\circ\text{F}$ ) and  $40\%$  relative humidity. The exterior climate is defined in Table 2. The exterior heat transfer coefficient is  $25 \text{ W}/\text{m}^2\cdot\text{K}$  (R-0.2  $\text{ft}^2\cdot\text{F}\cdot\text{h}/\text{Btu}$ ) with a wind-dependent vapor resistance. The wall is facing south with a rainwater absorption factor of  $0.1$ , i.e., a small amount of rain is available for capillary absorption. WUFI suggests  $0.7$  for most wall arrangements where the wall is fully exposed to the climate loads (Fraunhofer IBP 2010). In this case, the wall got fully saturated after a very short time period and no difference could be seen for the insulation cases. Therefore, a lower rainwater absorption factor was chosen for these simulations where  $10\%$  of the rain is available for capillary absorption and the remaining water runs down the façade or splashes off at impact. The results from the one-dimensional simulations of the four cases are shown in Figure 9.

As can be seen in Figure 9, adding a vapor barrier on the original brick wall does not change the total moisture content of the wall compared to the case without additional insulation. However, at the location  $60 \text{ mm}$  ( $2.4 \text{ in.}$ ) from the interior surface, the relative humidity is higher in the case of adding a vapor barrier than that without a vapor barrier, which indicates a lack of drying towards the interior space. This vapor transport is blocked when adding the vapor barrier.

In the two cases with thermal insulation installed on the interior surface of the brick wall, the moisture accumulation rate is higher than that of the original wall. With a vapor-open insulation, the moisture accumulation rate is slightly lower than for the case with VIP, which has a very high vapor resistance. Also, the relative humidity is slightly higher for the wall with VIP than for the wall with vapor-open insulation. The main part of the vapor and water flow in the wall is caused by the rain events and the indoor moisture content is of minor importance for the conditions studied here.

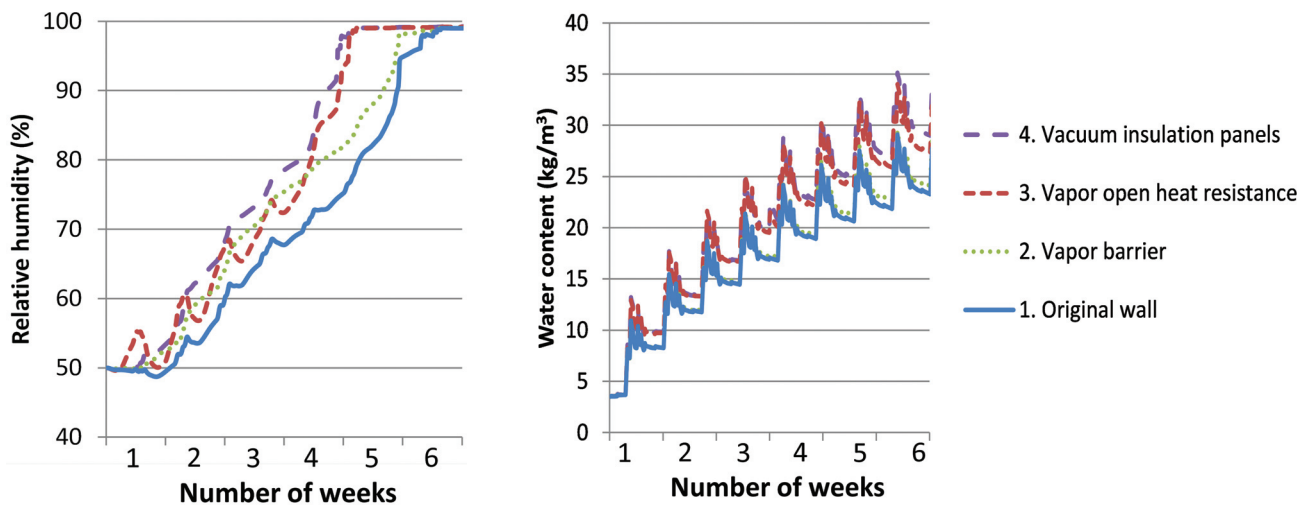


**Figure 9** Simulation of the relative humidity  $60 \text{ mm}$  ( $2.4 \text{ in.}$ ) from the interior surface and the total water content in the  $250 \text{ mm}$  ( $9.8 \text{ in.}$ ) wall composed of homogenous historical bricks and fine lime cement mortar between the bricks with varying interior boundary conditions during the climate cycle defined in Table 2.

## CONCLUSIONS

One- and two-dimensional hygrothermal simulations were used to investigate the relative humidity in a 250 mm (9.8 in.) thick brick wall. The purpose is to prepare an experimental benchmark in a laboratory environment where a brick wall with wooden beam ends is insulated with vacuum insulation panels (VIPs) on the interior. More specifically, the purpose is to estimate the influence of different brick and mortar types on the wetting and drying of the wall, to estimate the time scale of wetting, to estimate the rain load, and to investigate a possible reduction of the wall thickness from 380 mm (15 in.) to 250 mm (9.8 in.).

Two climate loads were investigated, where the Bergen, Norway, climate gave the highest moisture accumulation rate compared to the Gothenburg, Sweden, climate. The wall could be at risk of suffering freeze-thaw damage on the exterior surface in Bergen since the degree of saturation is close to the critical degree of saturation for some brick types. In Gothenburg, the wall did not reach as high a degree of saturation, but the number of freeze-thaw cycles was substantially higher.

The thickness of the wall influences the moisture accumulation rate when investigating the bricks 60 mm (2.4 in.) from the interior surface. The moisture accumulation rate does not decrease linearly with increasing thickness but has a more exponential relationship.

The moisture content in the wall is highly influenced by the properties of the brick. Two main groups of bricks were investigated, where hand-formed and historical bricks had similar properties while masonry and extruded bricks had similar properties. The time before the walls are saturated with moisture at the point 60 mm (2.4 in.) from the interior surface differed with a factor of 6 between the least and most permeable bricks.

The type of mortar influenced the drying of the wall during the investigated drying in a laboratory in the Trondheim, Norway, climate. The mortar that gave the lowest drying rate was the pure cement mortar, while the mixture of lime and cement gave a lower drying rate than pure lime mortar.

The properties of the interior insulation material were found to have a lesser influence on the moisture accumulation rate. The rain load is the dominating factor determining the vapor and water transport in the wall. Having the possibility of inward drying lowers the moisture accumulation rate slightly.

Based on the results from the numerical analysis, a 250 mm (9.8 in.) brick wall is proposed where the brick properties should resemble those of the brick type used in the early 20th century, i.e., a brick that is highly capillary active with a high liquid transport coefficient. The difference between using lime mortar and a lime cement mortar was not substantial; thus, lime cement mortar can be used in the laboratory tests. The rain load in the laboratory experiment should be limited so that the effect of the added interior VIP on the brick wall

and wooden beam ends is visible. With the results from the ongoing laboratory measurements, the influence of driving rain and solar radiation on a brick wall with interior VIP and wooden beam ends can be evaluated. The results can be used to refine the hygrothermal simulations so that more advanced simulations can be performed to draw more general conclusions of the applicability of VIPs in interior retrofitting of existing brick buildings. Using VIP, drying towards the interior is more limited and the only moisture transfer between the interior climate and the wall will be through the wooden beam ends and through possible cracks and air gaps between the VIP and at the beams. If the surface at the intermediate floor-to-wall attachment is left in its original state, moisture can also be transferred into the wall from here. In future studies these matters will be investigated numerically and compared to the results of the laboratory test.

## ACKNOWLEDGMENTS

The work is supported by the Swedish Research Council FORMAS, the Lars Hierta Memorial Foundation, the Research Council of Norway, and several partners through the Research Centre on Zero Emission Buildings ([www.ZEB.no](http://www.ZEB.no)).

## REFERENCES

- Abuku, M., Blocken, B., and Roels, S. 2009. Moisture response of building facades to wind-driven rain: Field measurements compared with numerical simulations. *Journal of Wind Engineering and Industrial Aerodynamics* 97(5-6):197–207.
- Angelantoni Industries S.p.A. n.d. Double room test equipment for building walls thermal performance testing Mod. UC2x18 RT/SR. Massa Martana, Italy: Angelantoni Industries S.p.A.
- Baetens, R., Jelle, B.P., Thue, J.V., Tenpierik, M.J., Grynning, S., Uvsløkk, S., and Gustavsen, A. 2010. Vacuum insulation panels for building applications: A review and beyond. *Energy and Buildings* 42(2):147–72.
- BIA. 2006. *Mortars for Brickwork—Selection and Quality Assurance*. Reston, Virginia, USA: The Brick Industry Association.
- Bjørberg, S., Lirhus, E.H., and Skattum, P. 2011. Vedlikehold-sveiledning: Murgårdsbebyggelsen i Oslo (Maintenance manual: Masonry buildings in Oslo). Oslo, Norway: Multiconsult AS.
- Boverket. 2009. Så mår våra hus – redovisning av regering-supplag beträffande byggnaders tekniska utformning m.m. (The state of our buildings – report of governmental mission on the technical design of buildings etc.). Karlskrona, Sweden: Boverket.
- Boverket. 2010. Energi i bebyggelsen - tekniska egenskaper och beräkningar – resultat från projektet BETSI (Energy in the built environment – technical properties and calculations – results from the BETSI study). Karlskrona, Sweden: Boverket.

- Brocken, H.J.P. 1998. Moisture transport in brick masonry: The grey area between bricks. Dissertation, Building Physics and Systems, Technische Universiteit Eindhoven, Eindhoven, The Netherlands.
- Brunner, S., and Simmler, H. 2008. In situ performance assessment of vacuum insulation panels in a flat roof construction. *Vacuum* 82(7):700–707.
- Brunner, S., Tharian, P.J., Simmler, H., and Ghazi Wakili, K. 2008. Focused ion beam (FIB) etching to investigate aluminium-coated polymer laminates subjected to heat and moisture loads. *Surface and Coatings Technology*, 202(24):6054–6063.
- CEN. 2007. EN 15026:2007, *Hygrothermal Performance of Building Components and Elements – Assessment of Moisture Transfer by Numerical Simulation*. Brussels: European Committee for Standardization.
- Hagentoft, C.-E., Kalagasidis, A.S., Adl-Zarrabi, B., Roels, S., Carmeliet, J., Hens, H., Grunewald, J., Funk, M., Becker, R., Shamir, D., Adan, O., Brocken, H., Kumaran, K., and Djebbar, R. 2004. Assessment method of numerical prediction models for combined heat, air and moisture transfer in building components: Benchmarks for one-dimensional cases. *Journal of Thermal Envelope and Building Science*, 27(4):327–52. <Benchmark files are available for download from [www.byggnadsteknologi.se/downloads.html](http://www.byggnadsteknologi.se/downloads.html)>
- Hall, C. 1977. Water movement in porous building materials—I. Unsaturated flow theory and its applications. *Building and Environment* 12(2):117–25.
- Hammett, M. 1997. *Resisting Rain Penetration With Facing Brickwork*. London, UK: The Brick Development Association.
- Fraunhofer IBP. 2010. WUFI 2D (Version 3.3.2) [Computer Program]. Holzkirchen, Germany: Fraunhofer IBP.
- Künzel, H. 1998. Effect of interior and exterior insulation on the hygrothermal behaviour of exposed walls. *Materials and Structures* 31(2):99–103.
- Kvande, T., and Edvardsen, K. I. 2007. Eldre yttervegger av mur og betong. Metoder og materialer. (Old exterior brick and concrete walls. Methods and materials). Building Research Design Guide 723.308. Oslo, Norway: SINTEF Byggeforsk.
- Mensinga, P., Straube, J., and Schumacher, C. 2010. Assessing the freeze-thaw resistance of clay brick for interior insulation retrofit projects. *Proceedings of the Thermal Performance of the Exterior Envelopes of Whole Buildings XI*, Clearwater Beach, FL, USA, December 5–9.
- Morelli, M., Scheffler, G.A., Nielsen, T.R., and Svendsen, S. 2010. Internal insulation of masonry walls with wooden floor beams in northern humid climate. *Proceedings of the Thermal Performance of the Exterior Envelopes of Whole Buildings XI*, Clearwater Beach, FL, USA, December 5–9.
- Nicolai, A., J. Grunewald, and H. Fechner. 2013. DELPHIN: Simulation program for the calculation of coupled heat, moisture, air, pollutant, and salt transport. Bauklimatik-Dresden, Germany.
- Piaia, J.C.Z., Cheriaf, M., Rocha, J.C., and Mustelie, N.L. 2013. Measurements of water penetration and leakage in masonry wall: Experimental results and numerical simulation. *Building and Environment* 61:18–26.
- Pfluger, R., Hasper, W., Schulze Darup, B., Sommer, D., and Forstner, M. 2008. Wissenschaftliche Analyse eines auf vorgefertigten Vakuum-Paneel-Verbundplatten beruhenden Innendämmsystems. Abschlussbericht (Scientific analysis of an interior insulation system based on prefabricated vacuum insulation composite panels. Final report). Neumarkt, Germany: VARIOTEC GmbH & Co.KG.
- Rasmussen, T.V. 2010. Post-insulation of existing buildings constructed between 1850 and 1920. *Proceedings of the Thermal Performance of the Exterior Envelopes of Whole Buildings XI*, Clearwater Beach, FL, USA, December 5–9.
- Straube, J., Ueno, K., and Schumacher, C. 2011. Internal insulation of masonry walls: Final measure guideline. Prepared for U.S. Department of Energy, Office of Energy Efficiency and Renewable Energy.
- Sveipe, E., Jelle, B.P., Wegger, E., Uvsløkk, S., Grynning, S., Thue, J.V., Time, B., and Gustavsen, A. 2011. Improving thermal insulation of timber frame walls by retrofitting with vacuum insulation panels—Experimental and theoretical investigations. *Journal of Building Physics* 35(2): 168–88.
- Thyholt, M., Pettersen, T.D., Haavik, T., and Wachenfeldt, B.J. 2009. Energy Analysis of the Norwegian Dwelling Stock. Subtask A—Internal working document. IEA SHC Task 37 Advanced Housing Renovation by Solar and Conservation.
- Wegger, E., Jelle, B.P., Sveipe, E., Grynning, S., Gustavsen, A., Baetens, R., and Thue, J.V. 2011. Aging effects on thermal properties and service life of vacuum insulation panels. *Journal of Building Physics* 35(2):128–67.